

Sonocatalytic Removal of Ciprofloxacin by Fe-Doped TiO_2 Nanoparticles from Aqueous Solution

Hossein Kamani

Zahedan University of Medical Sciences

Reza Haji Seyed Mohammad Shirazi

Islamic Azad University

Elham Norabadi

Zahedan University of Medical Sciences

Amir Hessam Hassani

Islamic Azad University

Abbas khalili (✉ khaliliamir96@gmail.com)

Islamic Azad University

Research Article

Keywords: Sonocatalytic process, Fe-doped TiO_2 , Ciprofloxacin, Sol-gel

Posted Date: April 19th, 2021

DOI: <https://doi.org/10.21203/rs.3.rs-400474/v1>

License: © ⓘ This work is licensed under a Creative Commons Attribution 4.0 International License.

[Read Full License](#)

Abstract

The present study was an experimental-laboratory study conducted as a batch system. Fe-doped TiO₂ nanoparticles were synthesized by the sol-gel method, and Scanning electron microscopy (SEM), X-ray diffraction (XRD), and Diffuse Reflectance Spectra (DRS) analyses were used to determine the properties of the synthesized nanoparticles. The effect of different variables including pH (3–9), initial concentration of ciprofloxacin (25–75 mg/L), and nanoparticle concentration (200–600 mg/L) at different times (15–60 minutes) was examined in sonocatalytic removal of ciprofloxacin. The results of this study disclosed that the maximum removal efficiency of ciprofloxacin is achievable at a pH of 9, initial concentration of ciprofloxacin 25 mg/L, and Fe-doped TiO₂ dose of 600 mg/L using ultrasound wave with a constant frequency of 35 kHz after 60 min. Therefore, due to the high efficiency of sonocatalytic removal, the employment of this process to remove ciprofloxacin and other antibiotics in water and wastewater treatment processes is recommended.

Highlights

- Iron doped Titanium Dioxide 2 wt.% and pure TiO₂ were prepared by sol-gel method
- Sonocatalytic process using Synthesized Fe-doped TiO₂ Nanoparticles shows a high ciprofloxacin degradation efficiency
- The influence of different parameters on the sonocatalytic removal of ciprofloxacin was investigated

1. Introduction

The presence of drug compounds, especially antibiotics, in the ecosystem has been known for more than a few decades. In recent years, the use of antibiotics in veterinary medicine and medical uses has widely increased (100,000 to 200,000 tons per year), and consequently, the possibility of contamination of water sources with such compounds has increased (Xu et al. 2007). Antibiotics enter aquatic environments through various pathways such as agricultural runoff, direct discharge from municipal treatment plants, human waste, direct disposal of medical, veterinary, and industrial wastes, etc. As a result, their presence has been observed in local streams and around the world, especially in streams that receive treated wastewater directly (Kitazono et al. 2012). These antibiotics are spread in the environment and can have important consequences for the ecosystem and human health. These compounds increase allergies in humans, increase bacterial resistance to antibiotics, upset the environmental balance, and unforeseen side effects on humans and animals (Al-Musawi et al. 2019; Kamani et al. 2017; Norabadi et al. 2020b; Rodayan et al. 2010).

Fluoroquinolones are one of the most potent groups of antibiotics used to treat urinary tract infections caused by gram-negative bacteria in humans and animals. Fluoroquinolones are very useful in the treatment of respiratory and urinary tract infections but have detrimental effects on the central nervous system, tendon toxicity, heart rate, tendon rupture, and hypoglycemia (Fink et al. 2012). Ciprofloxacin with

a chemical formula of $C_{17}H_{18}FN_3O_3$, molecular weight of 331.34 and solubility of 350 mg/L in water is one of the fluoroquinolone class antibiotics that is successfully used in the treatment of infections, especially urinary tract, respiratory and gastrointestinal infections(Ji et al. 2014; Wu et al. 2013).

There are various physical, chemical and biological methods such as chemical oxidation, biodegradation, adsorption, solvent extraction and membrane techniques to remove antibiotics that are selected according to the chemical and physical properties of the material. Because these compounds have been observed in effluents from wastewater treatment plants, conventional physical, chemical, and biological treatment can only degrade some of them(Esplugas et al. 2007). Degradation of these compounds is an important ecological challenge due to their complex structure and very low biodegradability(Lloret et al. 2010). Therefore, new processes with cost-effective methods are needed to treat such antibiotics, one of which is the sono-nanocatalyst process(Bautitz et al. 2007). The main mechanism of the ultrasonic process in the oxidation of pollutants is based on the formation of very small cavities or micro-bubbles that are the result of the sound cavitation phenomenon in water. The cavities created in the water have a temperature of 5000 K and a pressure of 1000 atmospheres, which eventually leads to the formation of OH and OOH radicals in the solution. The presence of these radicals in the water causes the oxidation of organic compounds(Mohammadi et al. 2011). Using the ultrasonic process alone requires high time and wave power. Therefore, semiconductor nanocatalysts such as ZnO, TiO_2 , etc. are used simultaneously with the application of ultrasonic waves in solution. TiO_2 nanoparticles are widely used due to their non-toxicity, cheapness, high chemical stability, and lack of secondary pollutants(Moradi et al. 2018; Tabasideh et al. 2017). However, due to the wide gap of the TiO_2 band (3.2 electron-volt) and its low quantum efficiency, they are severely limited(Lin et al. 2017). Nanocatalytic process modification methods include doping with metal ions (such as Mn^{2+} , Ni^{2+} , Zn^{2+} , Ag, Au, and Pt, Fe^{2+} , etc.), non-metallic ions (such as boron (B) and nitrogen (N)), sensitization with polymers and creating heterogeneity with other semiconductors, which has the best results among the above methods of doping with metal ions(Fei et al. 2015; Lin et al. 2017). In the metal ion doping method, among different types of metals, Fe^{3+} has been proposed as a suitable element for two reasons, i.e., the high similarity of Fe^{3+} radius (0.645 angstroms) to Ti^{4+} (0.604 angstroms) and easy connection to TiO_2 crystal lattice as well as inhibition of hole and electron recombination(Lin et al. 2017; Moradi et al. 2018). Removal of ciprofloxacin antibiotic from aqueous media using various oxidation and advanced oxidation methods such as ozonation process, photo-Fenton, photocatalyst, etc. has been studied, but no study on the sonocatalytic degradation of this antibiotic using Fe-doped TiO_2 nanoparticles has been conducted. The present study intends to investigate the effect of the sonocatalytic process using Fe-doped TiO_2 nanoparticles in removing ciprofloxacin as one of the resistant antibiotics.

2. Materials And Methods

In this study, ciprofloxacin from Sigma Aldrich Company was used to prepare the stock solution. Other chemicals used included tetraisopropyl orthotitanate ($C_{12}H_{28}O_4Ti$, $\geq 98\%$), nitric acid (HNO_3 , 65%), Iron

(III) nitrate nonahydrate ($\text{Fe}(\text{NO}_3)_3 \cdot 9\text{H}_2\text{O}$, $\geq 98\%$), 2-propanol ($\text{CH}_3\text{CH}(\text{OH})\text{CH}_3$), sulfuric acid (H_2SO_4 , 95-97%) and sodium hydroxide (NaOH , $\geq 98\%$) and were purchased from Merck, Germany.

2.1. Synthesis of Fe-doped TiO_2 and TiO_2 nanoparticles

In this study, the sol-gel method was used to synthesize Fe-doped TiO_2 and un-doped catalyst samples. To prepare the nanoparticles, a certain amount of iron nitrate with 2-propanol alcohol, deionized water, and nitric acid was poured into a flat bottom balloon and stirred for 15 minutes on a magnetic stirrer to mix thoroughly (solution No.1). In another balloon, a certain amount of titanium tetraisopropoxide and 2-propanol was mixed for 15 minutes to form a uniform and clear solution (solution No.2). Then, solution No.1 was added dropwise to the solution of container No.2, which was mixing on a magnetic stirrer. After mixing both solutions (solution NO.1 and No.2) and forming a clear cell inside the balloon, the balloon containing clear cell was left in the laboratory at room temperature for 5 hours and a semi-transparent gel was obtained, which had good resistance and adhesion. The resulting gel was placed in the oven at 80°C for 24 hours to dry. After that, the resulting dry powder was washed several times with double distilled water and was calcined in the oven at 500°C for one hour to prepare nano Fe-doped TiO_2 crystalline particles, and powder nanoparticles were obtained (Kamani et al. 2016).

2.2. Sonocatalytic analysis

The digital ultrasonic device (model: Elmasonic TI-H, Germany), with a frequency of 35 kHz, which was equipped with a stainless steel tank (with a useful volume of 3.5 liters and dimensions of $300 \times 340 \times 370$) was used. The desired concentrations of ciprofloxacin (25-50-75 mg/L) were prepared by diluting a certain amount of ciprofloxacin stock solution in a volume of 250 ml. The pH of the solutions was regulated in the desired pH range (3-5-7-9-11) using sodium hydroxide and sulfuric acid 0.1 and then a certain amount of synthesized Fe-doped TiO_2 catalyst (200-400-600 mg/L) was added to the solutions. Sampling was performed from the suspension irradiated with ultrasonic waves at the times of 15 to 60 minutes at different time intervals. After the oxidation process, the nanoparticles in the solution were separated from the solution by centrifugation at 4000 RPM and then the concentration of ciprofloxacin in the clarified clear solution was determined using a spectrophotometer and the removal efficiency was determined using the following formula.

$$\text{removal efficiency} = (C_0 - C_e) \times 100 / C_0 \quad (1)$$

3. Results And Discussion

3.1. Scanning electron microscopy (SEM) analysis

Scanning electron microscopy is a suitable tool for examining the morphology and appearance of synthesized nanoparticles. This device is useful for studying the particle shape and the approximate size

distribution of nanoparticles. Figure 1 shows the image of Fe-doped TiO₂ catalyst nanoparticles. As shown in Figure 1, the particles synthesized in the image are almost uniform, and no significant clogging are observed in them. The synthesized particles are very small and in the size of nanometers. The diameter of the synthesized particles is about 25-50 nm.

3.2. XRD analysis

In order to determine the crystal structure and estimate the size of the formed crystallites, X-ray diffraction (XRD) spectroscopy with a wavelength of 1.5418 Angstrom was used. Figure 2 shows the XRD spectrum of Fe-doped TiO₂ and un-doped TiO₂ nanoparticles at 2 θ of 10-80°.

The crystallite size in the synthesized nanoparticles was calculated using the Debye-Scherrer equation according to the following formula:

$$D = \frac{K\lambda}{\beta \cos\theta} \quad (2)$$

In the above formula, D is the average diameter of crystallite size (nm); K is crystal shape factor, which is usually constant and equal to 0.9; λ is X-ray wavelength used for XRD analysis (in this study, the wavelength is 1.5441 Angstrom); θ is diffraction angle in terms of degree, and β is the full-width at half maximum (FWHM).

As shown in Figure 2, the XRD spectra of samples of titanium dioxide doped with iron have large and sharp peaks that indicate good crystal structure in the synthesized nanoparticles. The peaks of 25.68, 37.75, 48.28, 54.27, and 55.24, which are marked inside the figure, confirm the crystal structure of the anatase phase.

Choi et al. studied the effect of different doping agents on the anatase to rutile phase transition and showed that the addition of small-radius doping agents could be integrated directly with the titanium dioxide crystal lattice to form a larger anatase phase. This phase has more oxidation power than other phases(Choi et al. 2009). As Figure 2 shows, the positions of the peaks on the X-axis are approximately the same, and no significant peaks were observed after the doping process in the Fe-doped nanoparticles, which confirms this point that the crystal structure of Fe-doped TiO₂ has not changed significantly. Eadi et al.(Eadi et al. 2017) also reported that the absence of a significant peak after the doping process could be due to iron values less than the detection limit or insensitivity of the device. On the other hand, due to the similarity of the ionic radii of Ti⁴⁺ (0.604 Angstrom) and Fe³⁺ (0.645 Angstrom), it is possible that a number of titanium dioxide lattice sites are occupied by iron ions(Moradi et al. 2018; Pang et al. 2012). Rahul Reddy et al.(Reddy et al. 2016) also concluded that the replacement of iron in the crystalline lattice of titanium dioxide could lead to a reduction in the rutile phase, which in turn could be due to the reduction of oxygen sites in the surface of titanium dioxide; this prevents the formation of other

crystalline phases. On the other hand, an increase in iron content can lead to changes in reflections at lower angles due to the replacement of Ti^{4+} ions with slightly larger Fe^{3+} ions. Kamani et al. (Kamani et al. 2016) in their study conducted for investigating the sonocatalytic removal of humic acid with doped titanium dioxide showed that the widening of the peaks and the change of reflections at lower angles can be due to the change of the absorption edge to the visible light region.

3.3. Diffuse Reflectance Spectra (DRS)

DRS analysis has been used to investigate the reduction in energy gap size after doping of doped elements in the structure of synthesized nanoparticles. Figure 3 shows the absorption spectra for the two samples synthesized in the wavelength range of 250-800 nm. In addition to determining the absorption spectrum, it is possible to quantitatively calculate the energy gap of nanoparticles by DRS analysis data and using the Kubelka-Munk Function and Tauc Method, followed by plotting $ah\nu^{1/2}$ graph against photon energy absorbed in terms of electron volts (hv).

$$(ah\nu) = A (h\nu - E_g)^r \quad (3)$$

In the above formula, a is the absorption coefficient; h is the planck's constant, ν is the light frequency, A is the absorption constant, E_g is the nanoparticle energy gap, and r is the optical transmission process.

Comparison of un-doped synthesized titanium dioxide nanoparticles with commercial titanium dioxide, which has an energy gap of 3.2 electron-volts, shows that nanoparticles synthesized by the sol-gel method have a lower energy gap. It can be due to the effective parameters during the synthesis of nanoparticles. Thus, the synthesized nanoparticles have a higher catalytic property than commercial titanium dioxide (Reddy et al. 2016; Sui et al. 2018).

According to Figure 3, the un-doped titanium dioxide nanoparticles did not show significant light absorption in the visible spectrum ($\lambda > 400$) and the absorption threshold for it was at the beginning of the visible wavelength wavelengths (401 nanometers). However, by doping iron in the structure of titanium dioxide, it has shifted the absorption wavelength to larger wavelengths and is closer to the visible light region. The reduction in band gap energy is also due to the action of the 3d orbital of titanium and the d orbital of iron, which placement of iron between titanium dioxide atoms in the structure of titanium dioxide leads to the production of an additional energy level between the valence band and the conduction band of titanium dioxide nanoparticles. The iron element doped in the structure of titanium dioxide acts as an intermediate energy level and reduces the energy gap and changes the absorption of light towards the visible region (Moradi et al. 2018; Pang et al. 2012; Sui et al. 2018).

As shown in Figure 4, after doping the elements to the titanium dioxide structure, its energy gap is reduced from 3.08 electron volts to 2.9 in Fe-doped TiO_2 samples. The reduction in the energy gap in Fe-doped titanium dioxide can be due to doping iron in the structure of titanium dioxide.

Therefore, according to the obtained results and the displacement of the energy gap from the ultraviolet to the visible light range, the energy required to excite the electron from the valence band to the conduction band and to perform the sonocatalytic reaction is reduced, and it is expected that the nanocatalyst synthesized in this study have more activity against ultrasound.

3.4. The effect of different parameters on the efficiency of ciprofloxacin sonocatalytic removal

3.4.1 Effect of different pH values of solution

In water and wastewater treatment, pH is an important factor in the removal of pollutants by adsorption and oxidation processes and, in most processes, has an important effect on the removal of pollutants. The pH through the adsorption of organic matter on the catalyst surface is an important factor in the photocatalytic and sonocatalytic degradation process because the process of photo/sonocatalytic degradation occurs more on the catalyst surface (Kamani et al. 2017).

Figure 5 shows the effect of pH on the ciprofloxacin degradation process at different acidic, neutral and, alkali levels at different times by keeping the other variables constant. As shown in Figure 5, the ciprofloxacin removal efficiency in acidic and very alkali is low. However, at alkaline pH values, the average efficiency has increased so that the highest removal efficiency has occurred at pH of 9.

The predominant surface charge of different types of catalysts in the natural state may be positive or negative, which is dependent on the surface properties, especially the surfactant groups and components of the catalyst. In sonocatalytic processes, pH_{zpc} plays an important role because, at pH_{zpc}, the positive and negative electrical charges on the surface of the catalyst are balanced. By increasing the pH to a value higher than pH_{zpc}, the dominant electric charge on the surface of the catalyst becomes negative, and by decreasing the pH below this point, the dominant electric charge on the surface of the catalyst becomes positive. The study of Kamani et al. showed that in sonocatalytic processes, the pH of the solution has an important effect on the production of hydroxyl radicals (strong oxidizing agents) (Kamani et al. 2017; Norabadi et al. 2020b). The pH_{zpc} for titanium dioxide is between 5.6 and 6.4. Therefore, the surface of Fe-doped TiO₂ catalyst is positive when pH < pH_{zpc}; it is negative for pH > pH_{zpc}, and it is neutral for pH = pH_{zpc}. Also, the structural properties of pollutants and intermediate products of oxidation will change with pH change (Liu et al. 2012).

The results obtained in this study are consistent with the results of the study of An et al. (An et al. 2010) for the degradation of ciprofloxacin using an advanced oxidation process, and, in this study, the highest reaction rate constant at pH 9 was 0.38 min⁻¹. The reason for these results is probably due to two effects: 1) the isoelectric point for titanium dioxide is approximately 6.3. Therefore, the surface of the iron-doped

titanium dioxide catalyst is positive when the pH is less than 6.4; it is negative when the pH is more than 6.4, and it is neutral when the pH is 6.4. 2) Ciprofloxacin is in three different ionic states, which mainly depends on the pH of the solution. The first degradation constant (pK_1) of ciprofloxacin is 6.15 ± 0.07 , and the second degradation constant (pK_2) is 8.66 ± 0.07 . Therefore, at the higher pH value, the molecules in the solution become more negative, and it is led to facilitate the adsorption of ciprofloxacin on the catalyst. In addition, under weak alkaline conditions and the presence of OH ions in solution, further hydroxyl radicals can be produced in solution. The reduction in the constant reaction rate at higher pH values may be due to the effect of repulsive forces and the reduction in adsorption of negatively charged ciprofloxacin onto the negatively charged catalyst bed, or it may be due to the scavenging role of hydroxyl in solution, which reduces radical production.

Gad-allah et al.(Gad-Allah et al. 2011) studied the photocatalytic oxidation of ciprofloxacin by simulated sunlight and obtained different results compared to the present study and reported that the maximum constant rate is for pH of 5.8, which is not the similar to the data obtained in this study. This difference may be due to the fact that they used ciprofloxacin hydrochloric acid instead of ciprofloxacin in their study.

3.4.2. Effect of initial concentration of ciprofloxacin

After determining the optimal pH in the previous step, the effect of the initial concentration of ciprofloxacin on the removal efficiency was investigated in this step. In this study, different initial concentrations of 25, 50, and 75 mg/L were considered, and the results were publicized in Figure 6. As shown in the figure, the removal efficiency of ciprofloxacin depends on the initial ciprofloxacin concentration. The maximum efficiency occurs at a lower concentration of pollutants and with increasing the concentration of pollutants, the removal efficiency decreases so that the maximum efficiency was achieved at a concentration of 25 mg/L, and the lowest efficiency was attained at a concentration of 75 mg/L. The results of this study were consistent with the results of Gul et al. and Iqbal et al. for the nanocatalytic degradation of Flumequine. They revealed that by increasing the concentration of contaminants in the solution, the degradation efficiency decreases. This decline in efficiency and reaction rate constant with increasing pollutant concentration can be due to the following reasons: 1) reducing the amount of active reactive species (such as hydroxyl radicals, etc.) for degradation of the target pollutant; 2) more competition between the target pollutant and intermediate products obtained from the degradation for hydroxyl radical reaction species, and 3) occupancy of active catalyst sites by intermediates and primary pollutant and consequently, reduction in radical production (Gul et al. 2020; Iqbal et al. 2020).

The results of various studies on sonocatalytic degradation of diazinon, tetracycline, and ciprofloxacin using nanocatalysts showed that increasing pollutant concentration enhances the removal efficiency and illuminated that this decrease in the efficiency is due to the occupation of nanocatalyst particles with

pollutant molecules, which inhibits the absorption of light on the surface of the catalyst and thus reduces the degradation efficiency (Hassani et al. 2017; Tabasideh et al. 2017).

According to the documentation on the effect of the initial concentration of ciprofloxacin on the degradation process, the decrease in degradation efficiency by the increasing ciprofloxacin concentration can be due to several reasons as follows: During the oxidation reaction, intermediates are formed by the degradation of ciprofloxacin, which at high concentrations, increases the competition between the primary ciprofloxacin molecules and the reaction intermediates to occupy the active sites on the nanocatalyst surface. Therefore, by occupying some active sites with intermediate products, fewer ciprofloxacin molecules can be substituted at active sites, thereby reducing efficiency. Another reason is that the hydroxyl radical reacts with both ciprofloxacin molecules and intermediates, and as a result, the degradation efficiency decreases when the initial concentration of ciprofloxacin increases. In addition, the amount of hydroxyl radical produced for the degradation process during the oxidation process is constant due to the constant concentration of Fe-doped TiO_2 nanocatalyst used in the solution while the concentration of ciprofloxacin increases; thus, the radicals produced in the solution for degradation of ciprofloxacin is not sufficient (Hassani et al. 2017; Lops et al. 2019).

3.4.3. Effect of different concentrations of Fe-doped TiO_2 nanoparticles

By determining the optimal pH and the initial effect of ciprofloxacin concentration in the previous steps, the removal efficiency of ciprofloxacin in different concentrations of Fe-doped TiO_2 catalyst was investigated in the next step. One of the most important parameters affecting the efficiency and optimal performance of hybrid processes and catalytic oxidation is the dose of catalytic nanoparticles used in the process (Norabadi et al. 2020a). Three different concentrations (200, 400, and 600 mg/L) were used to appraise the effect of Fe-doped TiO_2 concentration. Figure 7 shows the effect of different amounts of synthesized Fe-doped TiO_2 on the sonocatalytic removal of ciprofloxacin, and, as can be seen, the removal efficiency increased with increasing concentration of Fe-doped TiO_2 .

The study by Hosseini et al. for sonocatalytic degradation of tetracycline with different nanocatalyst values of 100 to 500 mg/L showed that by increasing the amount of nanocatalyst, the tetracycline degradation efficiency increases; they attributed this event to the increase in the number of available active sites and formation of greater hydroxyl radicals in solution, which can assist the tetracycline degradation efficiency. In addition, increasing the dose of nanoparticles leads to the presence of very fine particles in the solution to supply the nucleus to form cavitation bubbles and thus increase the production of more free radicals and increase the degradation efficiency (Hoseini et al. 2013).

ElShafei et al., Tabasideh et al., and Khan MAN et al. showed that increasing the concentration of nanocatalysts in solution leads to providing the additional surface area in the solution for cavitation

bubbles, which causes an increase in production of more free radicals in solution and improvement of efficiency (ElShafei et al. 2018; Tabasideh et al. 2017).

The study conducted by Gad-Allah et al. for the photocatalytic oxidation of ciprofloxacin by sunlight showed that increasing the concentration of nanocatalyst in solution, up to an optimal amount, enhances the effective surface area exposed to light for more production of free radicals. On the other hand, the addition of nanocatalyst develops the number of active sites for the adsorption of ciprofloxacin (Gad-Allah et al. 2011).

4. Conclusion

This study was performed to estimate the sonocatalytic oxidation efficiency of ciprofloxacin antibiotic from aqueous media by Fe-doped TiO₂ nanoparticles. The particles synthesized by the sol-gel method were very fine and in the range of 25–50 nm. Different analyzes of synthesized nanoparticles showed that nanoparticles have good uniformity and dispersion. In XRD analysis, large and sharp formed peaks confirmed the good crystal structure of the synthesized nanoparticles. Doping iron in the structure of titanium dioxide reduced the energy gap of titanium dioxide from 3.08 to 2.9. Doping was also led to shifting the absorption wavelength to higher wavelengths and closer to the visible region. The maximum removal efficiency of ciprofloxacin using ultrasound wave (frequency of 35 kHz) was obtained at optimal conditions, e.g., pH of 9, initial ciprofloxacin concentration of 25 mg/L, and Fe-doped TiO₂ nanoparticles dose of about 600 mg/L at 60 min reaction time. Therefore, due to the high efficiency of the sonocatalytic process, the use of this process to remove ciprofloxacin in complimentary water and wastewater treatment processes is recommended.

Declarations

Acknowledgment

This article is the result of a part of the Ph.D. which has been implemented with the support of the Islamic Azad University, Science and Research Branch. Hereby, the authors appreciate the Islamic Azad University, Science and Research Branch for the financial support of this research.

Funding

The authors appreciate the Islamic Azad University, Science and Research Branch for the financial support of this research.

Conflicts of interest/Competing interests

The authors declare that they have no competing interests.

Data availability

All data generated or analysed during this study are included in this published article (and its supplementary information files).

Authors' contributions

All authors contributed to the study conception and design. Writing - original draft preparation, Material preparation, data collection and analysis were performed by [Hossein Kamani], [Abbas khalili] and [Elham Norabadi], review and editing by [Hossein Kamani], [Reza Haji Seyed Mohammad Shirazi], [Amir Hessam Hassani]. All authors read and approved the final manuscript.

References

1. Al-Musawi TJ, Kamani H, Bazrafshan E, Panahi A H, Silva MF, Abi G (2019) Optimization the effects of physicochemical parameters on the degradation of cephalexin in sono-Fenton reactor by using box-Behnken response surface methodology. *Catal Lett* 149:1186–1196. <https://doi.org/10.1007/s10562-019-02713-x>
2. An T, Yang H, Li G, Song W, Cooper WJ, Nie X (2010) Kinetics and mechanism of advanced oxidation processes (AOPs) in degradation of ciprofloxacin in water. *Appl Catal B Environ* 94:288–294
3. Bautitz IR, Nogueira RFP (2007) Degradation of tetracycline by photo-Fenton process—Solar irradiation and matrix effects. *J Photochem Photobiol A Chem* 187:33–39. <https://doi.org/10.1016/j.apcatb.2009.12.002>
4. Choi J, Park H, Hoffmann MR (2009) Effects of single metal-ion doping on the visible-light photoreactivity of TiO₂. *J Phys Chem C* 114:783–792. <https://doi.org/10.1021/jp908088x>
5. Eadi SB, Kim S, Jeong SW, Jeon HW (2017) Novel Preparation of Fe Doped TiO₂ Nanoparticles and Their Application for Gas Sensor and Photocatalytic Degradation. *Advanc Mater Sci Eng* 2017. <https://doi.org/10.1155/2017/2191659>
6. Elshafei GM, Al-Sabagh A, Yehia F, Philip C, Moussa N, Eshaq G, Elmetwally A (2018) Metal oxychlorides as robust heterogeneous Fenton catalysts for the sonophotocatalytic degradation of 2-nitrophenol. *Appl Catal B Environ* 224:681–691. <https://doi.org/10.1016/j.apcatb.2017.11.015>
7. Esplugas S, Bila D M, Krause LG, T, Dezotti M (2007) Ozonation and advanced oxidation technologies to remove endocrine disrupting chemicals (EDCs) and pharmaceuticals and personal care products (PPCPs) in water effluents. *J Hazard Mater* 149:631–642. <https://doi.org/10.1016/j.jhazmat.2007.07.073>
8. Fei J, Li J (2015) Controlled preparation of porous TiO₂–Ag nanostructures through supramolecular assembly for plasmon-enhanced photocatalysis. *Adv Mater* 27:314–319. <https://doi.org/10.1002/adma.201404007>
9. Fink L, Dror I, Berkowitz B (2012) Enrofloxacin oxidative degradation facilitated by metal oxide nanoparticles. *Chemosphere* 86:144–149. <https://doi.org/10.1016/j.chemosphere.2011.10.002>

10. Gad-Allah T, A, Ali MEM, Badawy MI (2011) Photocatalytic oxidation of ciprofloxacin under simulated sunlight. *J Hazard Mater* 186:751–755. <https://doi.org/10.1016/j.jhazmat.2010.11.066>
11. Gul I, Sayed M, Shah NS, Ali Khan J, Polychronopoulou K, Iqbal J, Rehman F (2020) Solar light responsive bismuth doped titania with Ti^{3+} for efficient photocatalytic degradation of flumequine: Synergistic role of peroxymonosulfate. *Chem Eng J* 384:123255. <https://doi.org/10.1016/j.cej.2019.123255>
12. Hassani A, Khataee A, Karaca S, Karaca C, Gholami P (2017) Sonocatalytic degradation of ciprofloxacin using synthesized TiO_2 nanoparticles on montmorillonite. *Ultrason Sonochem* 35:251–262. <https://doi.org/10.1016/j.ultsonch.2016.09.027>
13. Hoseini M, Safari GH, Kamani H, Jaafari J, Ghanbarain M, Mahvi AH (2013) Sonocatalytic degradation of tetracycline antibiotic in aqueous solution by sonocatalysis. *Toxicol Environ Chem* 95:1680–1689. <https://doi.org/10.1080/02772248.2014.901328>
14. Iqbal J, Shah NS, Sayed M, Muhammad N, Rehman S-U, Khan JA, Haq Khan Z, U, Howari FM, Nazzal Y, Xavier C, Arshad S, Hussein A, Polychronopoulou K (2020) Deep eutectic solvent-mediated synthesis of ceria nanoparticles with the enhanced yield for photocatalytic degradation of flumequine under UV-C. *J Water Process Eng* 33:101012. <https://doi.org/10.1016/j.jwpe.2019.101012>
15. Ji Y, Ferronato C, Salvador A, Yang X, Chovelon J-M (2014) Degradation of ciprofloxacin and sulfamethoxazole by ferrous-activated persulfate: implications for remediation of groundwater contaminated by antibiotics. *Sci Total Environ* 472:800–808. <https://doi.org/10.1016/j.scitotenv.2013.11.008>
16. Kamani H, Bazrafshan E, Ashrafi SD, Sancholi F (2017) Efficiency of sono-nano-catalytic process of TiO_2 nano-particle in removal of erythromycin and metronidazole from aqueous solution. *J Mazandaran Univ Med Sci* 27:140–154
17. Kamani H, Nasser S, Khoobi M, Nodehi RN, Mahvi AH (2016) Sonocatalytic degradation of humic acid by N-doped TiO_2 nano-particle in aqueous solution. *J Environ Health Sci Eng* 14:3. <https://doi.org/10.1186/s40201-016-0242-2>
18. Kitazono Y, Ihara I, Yoshida G, Toyoda K, Umetsu K (2012) Selective degradation of tetracycline antibiotics present in raw milk by electrochemical method. *J Hazard Mater* 243:112–116. <https://doi.org/10.1016/j.jhazmat.2012.10.009>
19. Lin L, Wang H, Jiang W, Mkaouer AR, Xu P (2017) Comparison study on photocatalytic oxidation of pharmaceuticals by TiO_2 -Fe and TiO_2 -reduced graphene oxide nanocomposites immobilized on optical fibers. *J Hazard Mater* 333:162–168. <https://doi.org/10.1016/j.jhazmat.2017.02.044>
20. Liu L, Chen F, Yang F, Chen Y, Crittenden J (2012) Photocatalytic degradation of 2,4-dichlorophenol using nanoscale Fe/ TiO_2 . *Chem Eng J* 181–182:189–195. <https://doi.org/10.1016/j.cej.2011.11.060>
21. Lloret L, Eibes G, Lú-Chau T, Moreira M, Feijoo G, Lema J (2010) Laccase-catalyzed degradation of anti-inflammatories and estrogens. *Biochem Eng J* 51:124–131.

<https://doi.org/10.1016/j.bej.2010.06.005>

22. Lops C, Ancona A, Di Cesare K, Dumontel B, Garino N, Canavese G, Hernández S, Cauda V (2019) Sonophotocatalytic degradation mechanisms of Rhodamine B dye via radicals generation by micro- and nano-particles of ZnO. *Appl Catal B Environ* 243:629–640.
<https://doi.org/10.1016/j.apcatb.2018.10.078>
23. Moradi V, Jun MB, Blackburn A, Herring RA (2018) Significant improvement in visible light photocatalytic activity of Fe doped TiO₂ using an acid treatment process. *Appl Surf Sci* 427:791–799. <https://doi.org/10.1016/j.apsusc.2017.09.017>
24. Norabadi E, Ashrafi SD, Kamani H, Jahantig A (2020a) Degradation of 2, 6-dichlorophenol by Fe-doped TiO₂ Sonophotocatalytic process: kinetic study, intermediate product, degradation pathway. *Int J Environ Anal Chem* 1–16. <https://doi.org/10.1080/03067319.2020.1837122>
25. Norabadi E, Panahi AH, Ghanbari R, Meshkinian A, Kamani H, Ashrafi SD (2020b) Optimizing the parameters of amoxicillin removal in a photocatalysis/ozonation process using Box-Behnken response surface methodology. *Desalination Water Treat* 192:234–240.
[doi:10.5004/dwt.2020.25728](https://doi.org/10.5004/dwt.2020.25728)
26. Pang YL, Abdullah AZ (2012) Effect of low Fe³⁺ + doping on characteristics, sonocatalytic activity and reusability of TiO₂ nanotubes catalysts for removal of Rhodamine B from water. *J Hazard Mater* 235:326–335. <https://doi.org/10.1016/j.jhazmat.2012.08.008>
27. Reddy DR, Dinesh GK, Anandan S, Sivasankar T (2016) Sonophotocatalytic treatment of Naphthol Blue Black dye and real textile wastewater using synthesized Fe doped TiO₂. *Chem Eng Process: Process intensif* 99:10–18. <https://doi.org/10.1016/j.cep.2015.10.019>
28. Rodayan A, Roy R, Yargeau V (2010) Oxidation products of sulfamethoxazole in ozonated secondary effluent. *J Hazard Mater* 177:237–243. <https://doi.org/10.1016/j.jhazmat.2009.12.023>
29. Sui Y, Liu Q, Jiang T, Guo Y (2018) Synthesis of nano-TiO₂ photocatalysts with tunable Fe doping concentration from Ti-bearing tailings. *Appl Surf Sci* 428:1149–1158.
<https://doi.org/10.1016/j.apsusc.2017.09.197>
30. Tabasideh S, Maleki A, Shahmoradi B, Ghahremani E, McKay G (2017) Sonophotocatalytic degradation of diazinon in aqueous solution using iron-doped TiO₂ nanoparticles. *Sep Purif Technol* 189:186–192. <https://doi.org/10.1016/j.seppur.2017.07.065>
31. Wu S, Zhao X, Li Y, Zhao C, Du Q, Sun J, Wang Y, Peng X, Xia Y, Wang Z (2013) Adsorption of ciprofloxacin onto biocomposite fibers of graphene oxide/calcium alginate. *Chem Eng J* 230:389–395. <https://doi.org/10.1016/j.cej.2013.06.072>
32. Xu W-H, Zhang G, Zou S-C, Li X-D, Liu Y-C (2007) Determination of selected antibiotics in the Victoria Harbour and the Pearl River, South China using high-performance liquid chromatography-electrospray ionization tandem mass spectrometry. *Environ Pollut* 145:672–679.
<https://doi.org/10.1016/j.envpol.2006.05.038>

Figures

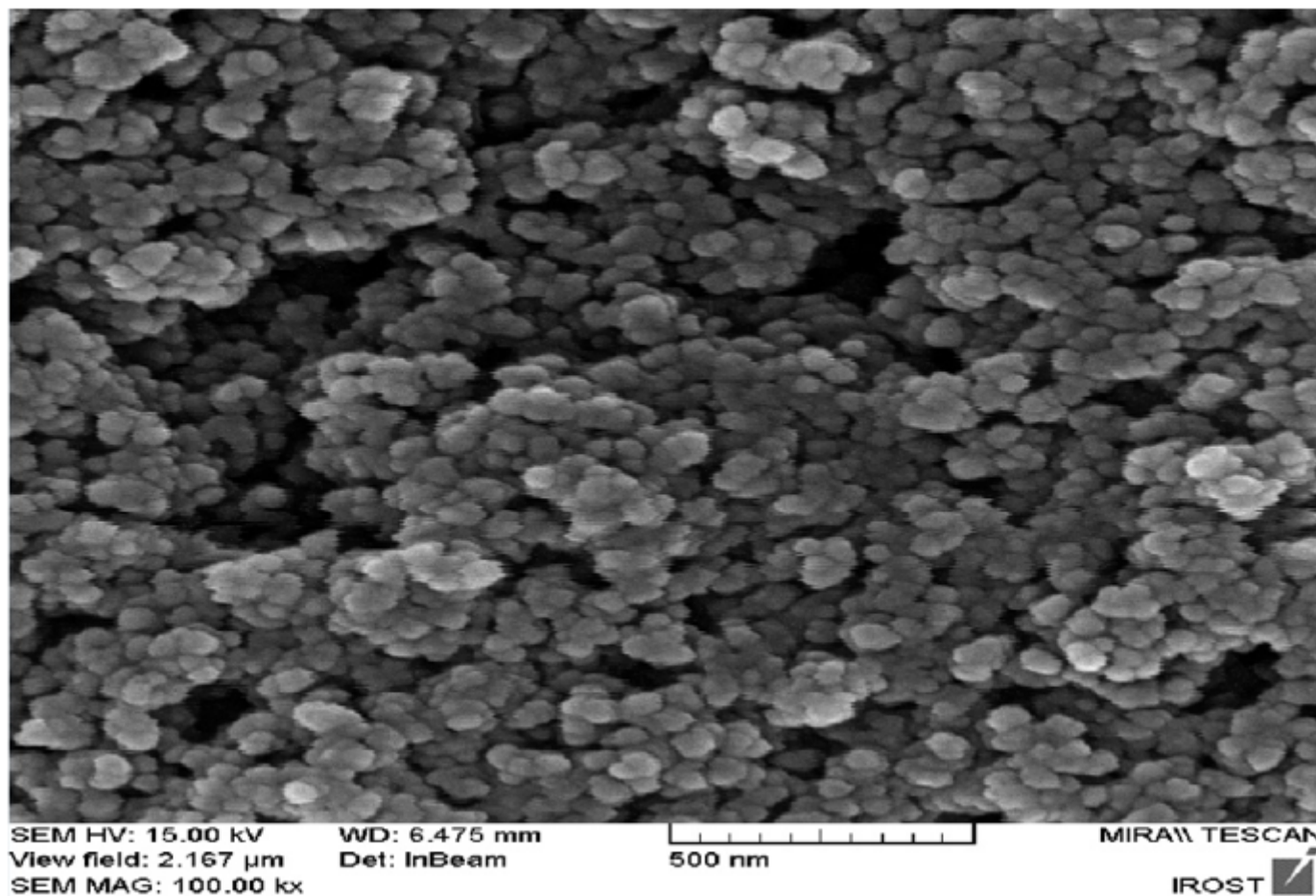


Figure 1

SEM image of synthesized Fe-doped TiO₂ nanoparticles

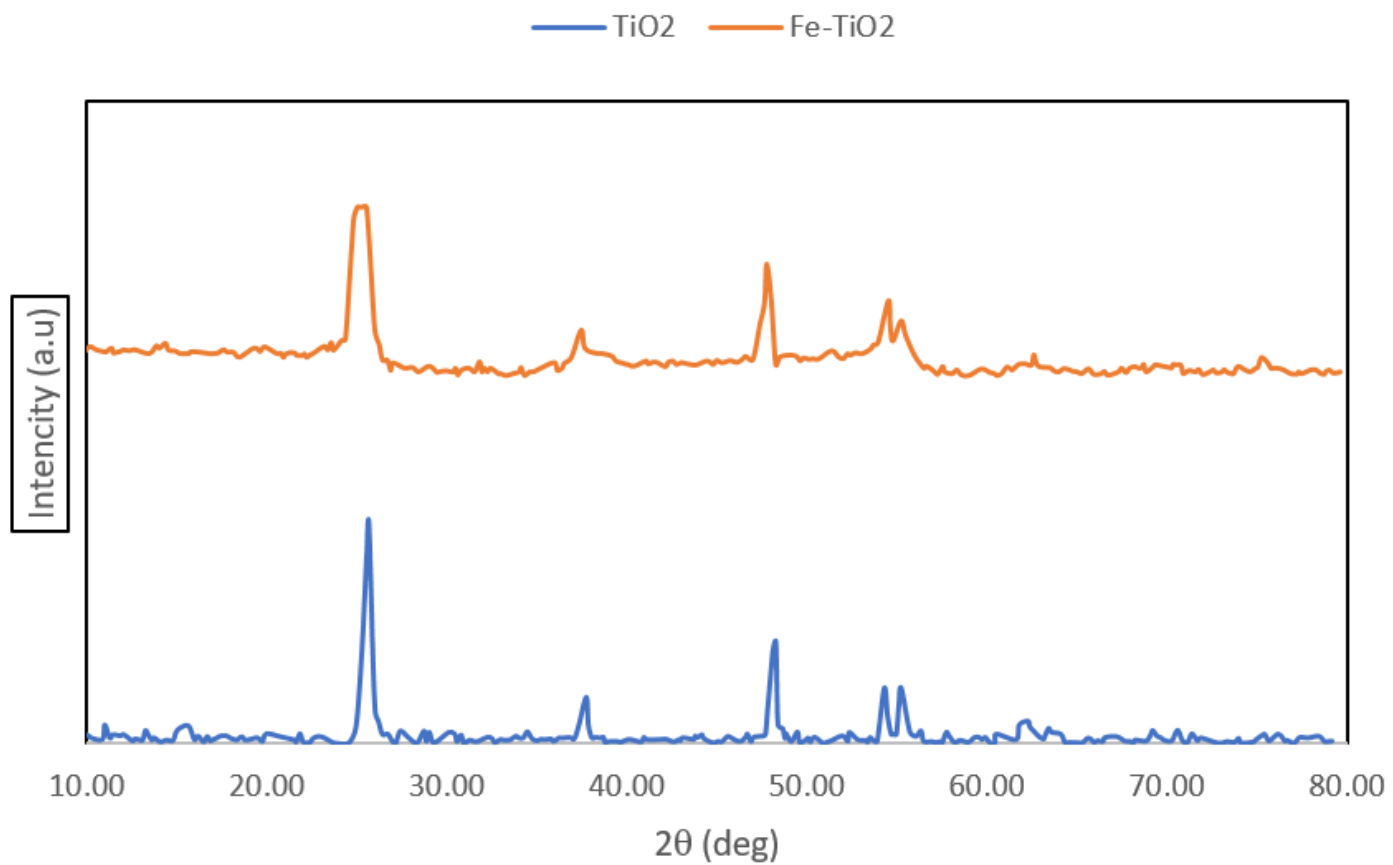


Figure 2

XRD pattern of un-doped and Fe-doped TiO_2 nanoparticles

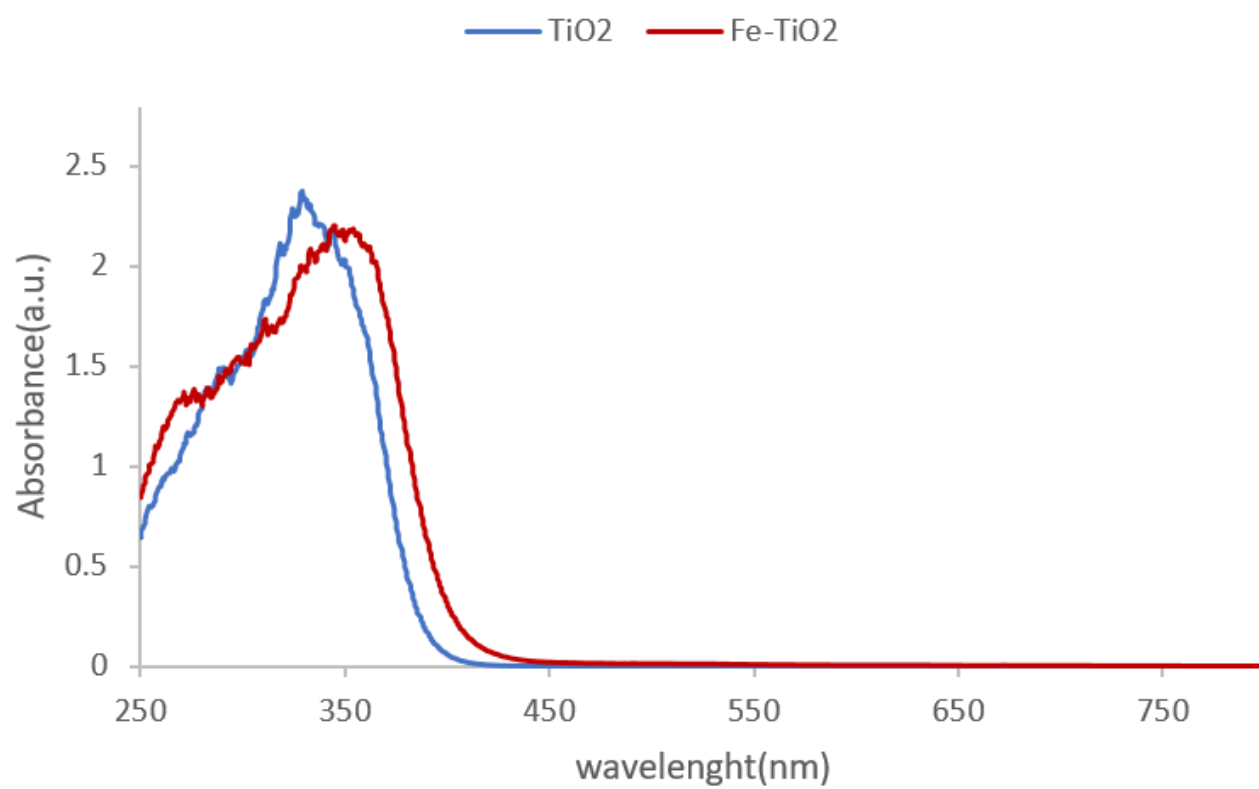


Figure 3

UV-Vis Diffuse Reflectance Spectra

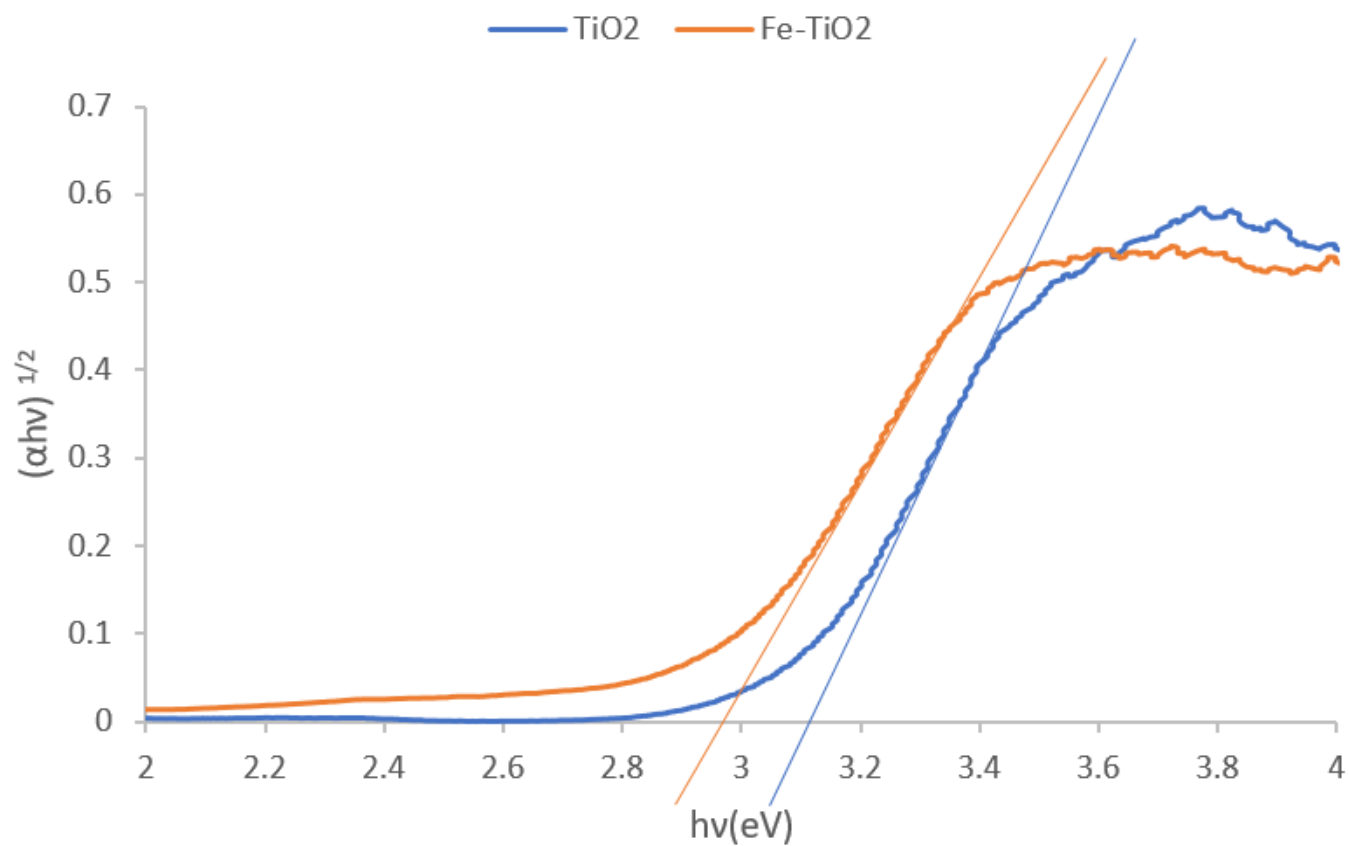


Figure 4

Reduction of band gap of un-doped and Fe-doped TiO₂

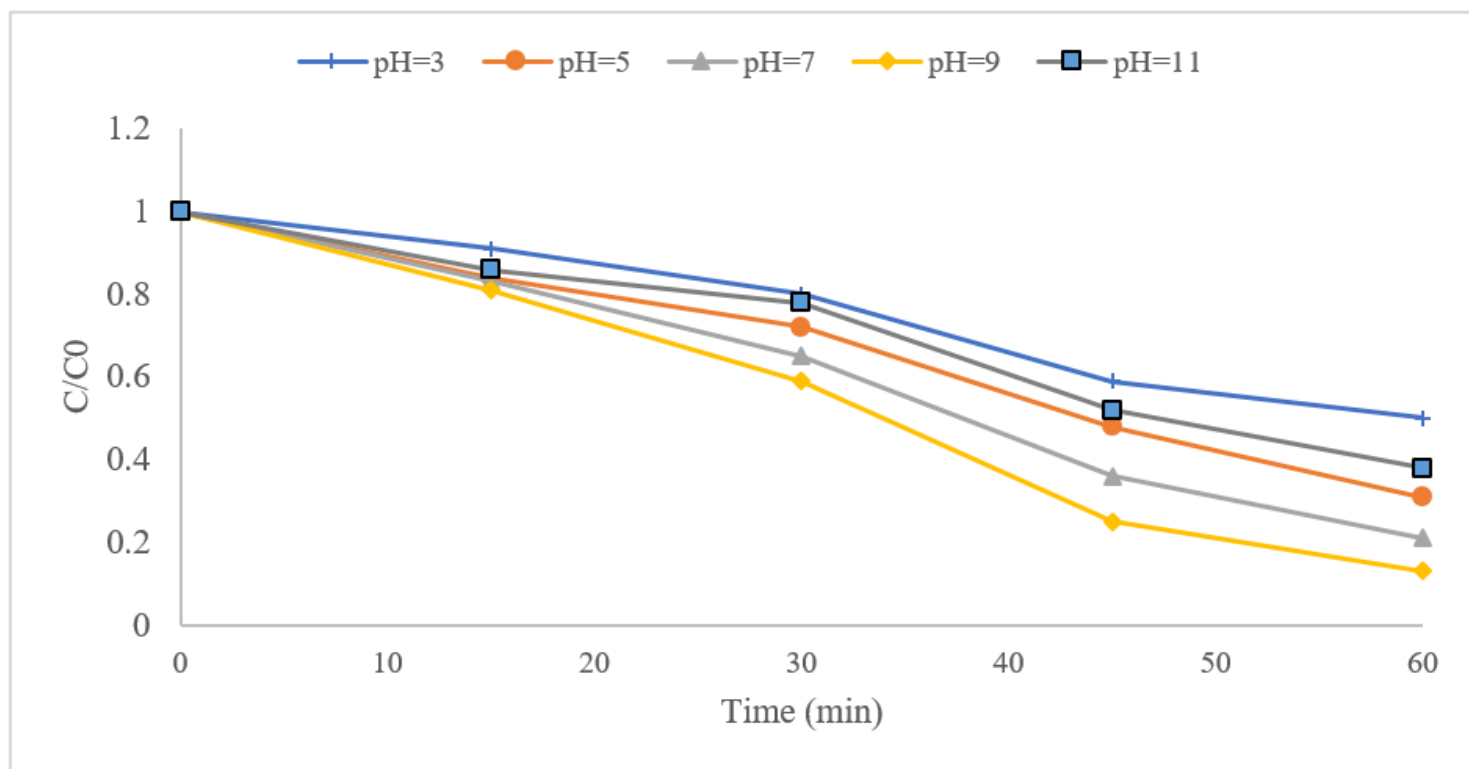


Figure 5

Effect of initial pH on sonocatalytic removal (ciprofloxacin con:50 mg L⁻¹ , Fe-doped TiO₂ con:400 mg L⁻¹)

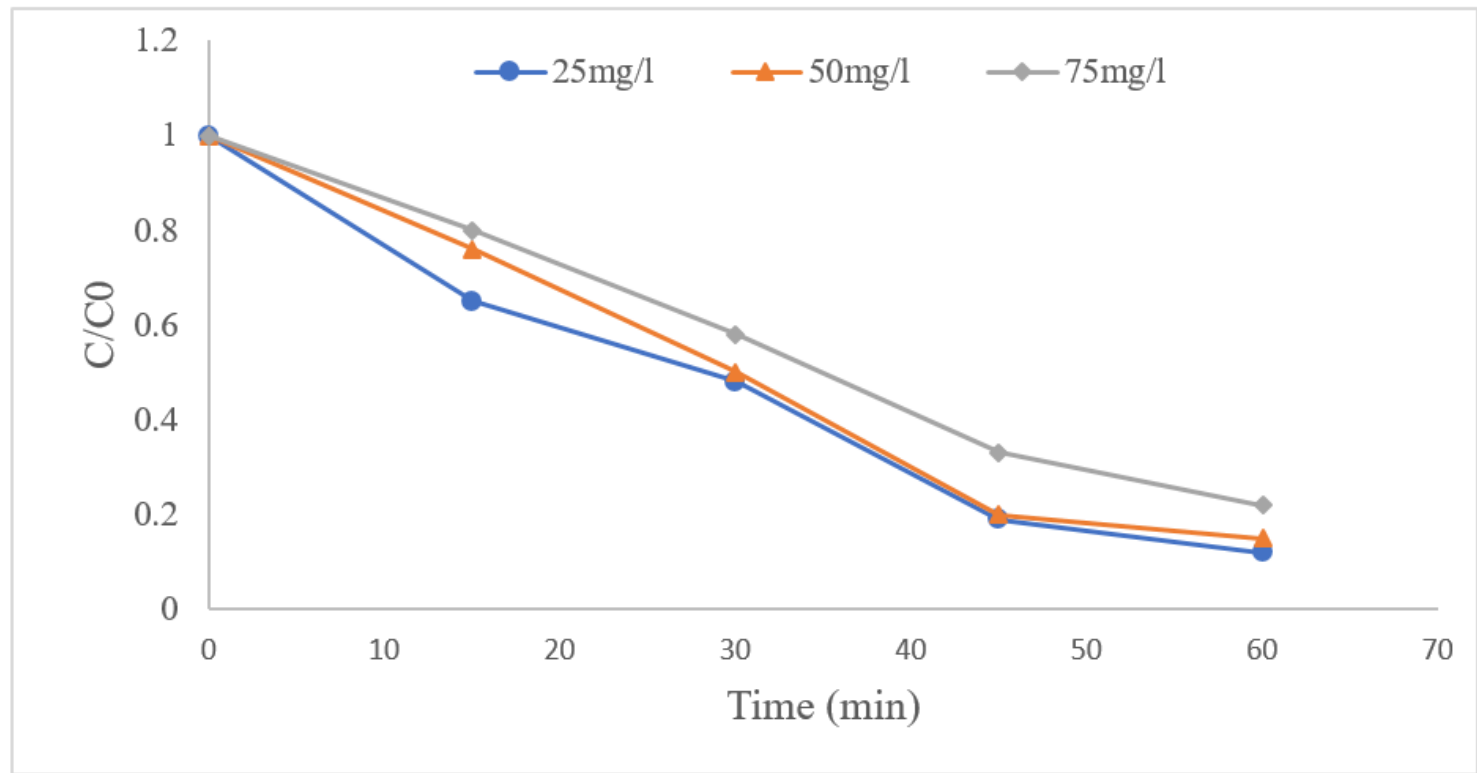


Figure 6

Effect of initial ciprofloxacin concentration on sonocatalytic removal (pH:9, Fe-doped TiO₂ con:400 mg L⁻¹)

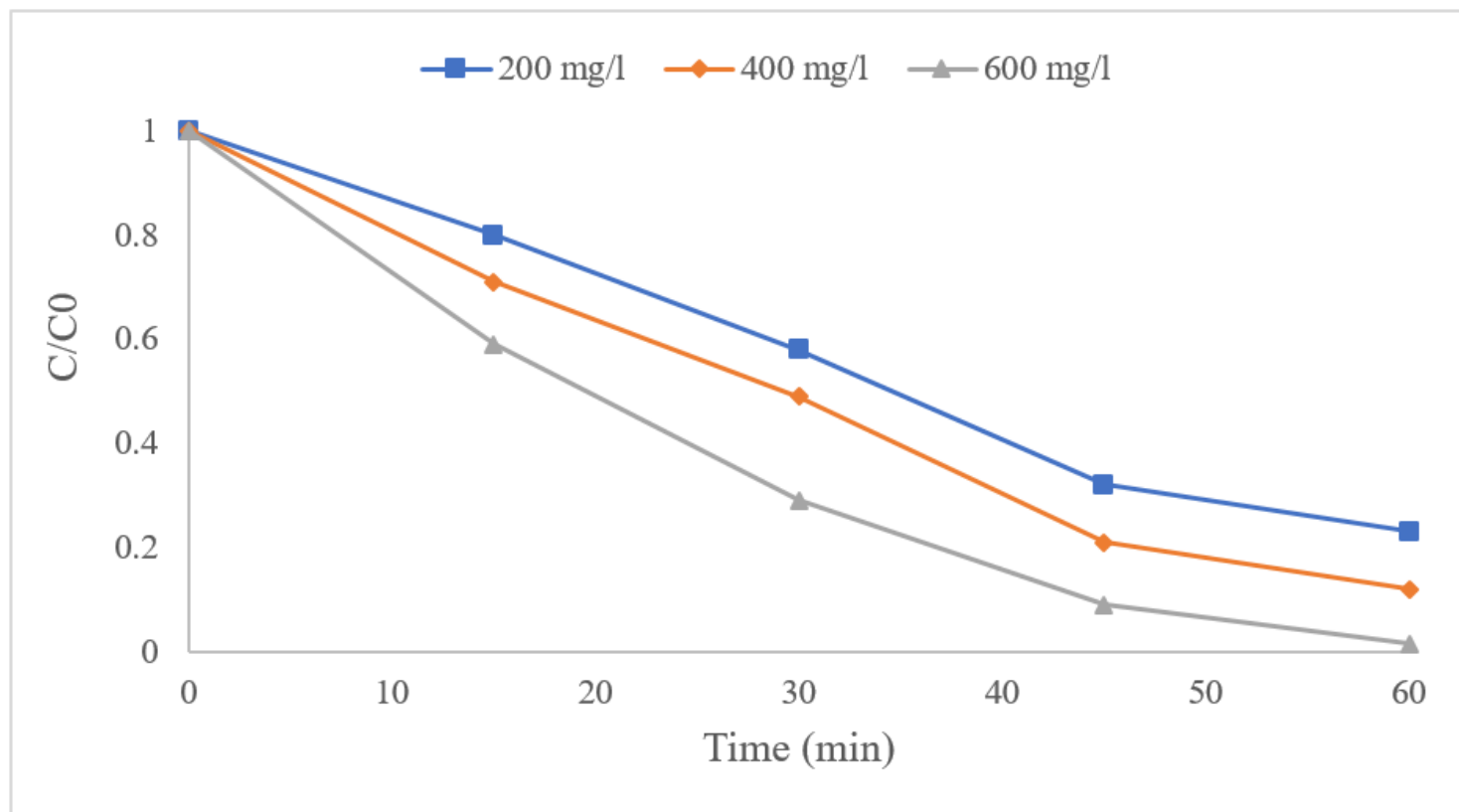


Figure 7

Effect of Fe-doped TiO₂ concentration on sonocatalytic removal (pH:9, ciprofloxacin con:25 mg L⁻¹)